Thermochimica Acta, 181 (1991) 1–11
Elsevier Science Publishers B.V., Amsterdam

CALORIMETRY AND X-RAY DIFFRACTION INVESTIGATIONS OF THE BINARY SYSTEM NEOPENTYLGLYCOL–PENTAERYTHRITOL

M. TEISSEIRE

Laboratoire de Physique du Solide et d'Energie Solaire, CNRS, Av. B. Gregory, 06560 Valbonne (France)

N.B. CHANH

Laboratoire de Cristallographie et de Physique Cristalline, URA 144 CNRS Université de Bordeaux I, Talence (France)

M.A. CUEVAS-DIARTE

Departament de Fisica i Enginyeria Nuclear, Universitat Politècnica de Catalunya 08028 Barcelona (Spain)

J. GUION

Laboratoire de Physique du Solide et d'Energie Solaire, CNRS, Av. B. Gregory, 06560 Valbonne (France)

Y. HAGET

Laboratoire de Cristallographie et de Physique Cristalline, URA 144 CNRS Université de Bordeaux I, Talence (France)

D. LOPEZ and J. MUNTASELL

Departament de Cristallografia, Universitat de Barcelona (Spain)

(Received 18 July 1990)

ABSTRACT

Experimental measurements, mainly differential scanning calorimetry (DSC) and variable-temperature X-ray spectra (Guinier–Simon) are presented for different compositions (X_{PE}) of the binary system pentaerythritol–neopentylglycol. Calorimetric results are analysed through the "shape factors method", and compared to those of X-ray recordings, allowing the presentation of the unusually complicated phase diagram proposed here, with the presence of metatectic, peritectic and eutectoïd invariants.

INTRODUCTION

Successive substitutions of $-CH_3$ groups in neopentane $C(CH_3)_4$ by $-CH_2OH$ groups give rise to a series of polyols well known to belong in the solid state to the class of plastic crystals [1].

Neopentylglycol (NPG), $(CH_3)_2C(CH_2OH)_2$, pentaglycerin (PG), $(CH_3)C(CH_2OH)_3$ and pentaerythritol (PE), $C(CH_2OH)_4$ are "globular molecules", and undergo solid–solid phase transition from an anisotropic low temperature phase to a high temperature isotropic phase called the "plastic phase". These transitions are very energetic, related to a large entropy variation ΔS_{tr} compared to the solid–liquid transition ΔS_m.

Recently, several investigations [2–5] concerned the study of the solid–solid phase transition mechanism. In the plastic solid phase, molecules are allowed to present several possible orientations on a given crystallographic site configuration associated with weak potential energy barriers between the different orientations. The plastic phase is highly symmetric, f.c.c. for the polyols studied here.

Owing to the large enthalpy variation observed during the crystal plastic phase transition, these compounds and some substituted derivatives were investigated for their potential use in thermal energy storage systems [6–9].

Staveley [10] pointed out that mixtures of this type of compound should lead to extended solid solutions in the plastic phase, but very few phase diagram determinations have been performed until recently. The work of Benson et al. [9,11] covered part of the binary systems PE–PG and PE–NPG, but called for more and deeper examination. A systematic investigation of "molecular alloy" formation undertaken by the Reseau Européen des Alliages Moléculaires (REALM) group, has led to recent proposals of phase diagrams for PE–PG [12], PE–NPG [13] and PG–NPG [14] binary systems.

The binary system (PE–NPG) study presented here is a first report of results showing an unexpectedly complicated situation. A large number of experimental determinations, including differential scanning calorimetry (DSC) and temperature variable X-ray (Guinier–Simon) measurements, are discussed and lead to the present phase diagram proposition.

EXPERIMENTAL

Thermal analysis with DSC

Thermograms were recorded with a SETARAM DSC 111 apparatus. Sample masses used were of the order of 90–110 mg. The weighted sample was introduced in an inox crucible, hermetically sealed with an inox cap and aluminium gasket. The rate of heating was taken as 1 K min^{-1}. Each experiment was first run with the empty crucible cap and gasket, and the thermal results for this blank were then substracted for the experiment with the filled capped and sealed crucible.

In many runs we recorded both $dQ/dT = f(T)$ curves for the heating and then for the cooling mode. For each concentration, at least two different experiments were done. For some concentrations, successive cycles (heating

and cooling on the sample) were recorded. In a few cases, the observation of non-reproducibility of recorded thermograms led to a careful analysis of the influence of the preparation of samples.

Crystallographic investigations

Guinier–Hagg method

Guinier–Hagg method has been used on powdered samples at ambient temperature for pure compounds and several binary mixtures at different concentrations. We have thus shown the existence of a large demixtion domain.

X-ray studies

The Guinier–Simon X-ray camera allows the continuous evolution of the diffraction pattern of a sample with temperature to be followed on film. The experimental conditions were Cu $K\alpha_1$ radiation, quartz monochromator, window width of 1.5 mm, and film displacement speed of 2 mm h^{-1}. The heating rate used was 0.2 K min^{-1}, and then temperature interval explored ranged from 293 K to melting temperatures of studied mixtures, previously determined from DSC experiments.

The sample was introduced in Lindemann tubes, the remaining empty space of which was filled with quartz powder, in order to limit any condensation effect in the cold top part, linked to possible sublimation of one of the components (NPG is more sublimable than PE).

Sample preparation

Pure compounds (PE 98%, NPG 97%) were purchased from Aldrich Chemical Co. After recrystallisation and drying for PE, and vacuum sublimation for NPG, the different mixed samples were prepared by weighing PE and NPG in the desired proportions. The two components were finely ground and then introduced into a glass cell, which was sealed before introduction into a furnace. The mixture was then melted and stirred, avoiding overheating which may result in some decomposition of material. The sample was finally allowed to cool very slowly (10 K h^{-1}) in the furnace, in order to avoid freezing of metastable phases commonly observed otherwise.

EXPERIMENTAL RESULTS AND DATA TREATMENT

The whole thermograms may be coherently analysed using the "shape factors" method developed by Courchinoux et al. [15]. The basis of this method was analysed through an experimental study of the main parameters

which influence the shape of a thermal signal. In the case of an isothermal phenomenon (for instance, the melting of a pure material at a temperature T) the thermal signal appears to begin effectively [16] at $T = T_o$ (onset temperature); its summit is at T_S and it finishes at T_{fin}.

$\Delta T_S = T_S - T_0$ and $\Delta T_{fin} = T_{fin} - T_0$ are two shape factors. The authors have shown that ΔT_S and ΔT_{fin} can be considered as quasi-constant for all the compounds of a given family provided that all the experimental conditions remain the same (i.e. device, mass, measurement cells, atmosphere, heating rate etc.) so that the temperature of the phenomenon can be reached as

$$T = T_0 = T_S - (\Delta T_S)_0 = T_{fin} - (\Delta T_{fin})_0$$

where $(\Delta T_S)_0$ and $(\Delta T_{fin})_0$ are characteristic values of the series.

The authors show how to use $(\Delta T_S)_0$ and $(\Delta T_{fin})_0$ to determine the actual characteristic temperatures of a binary phase diagram, i.e. when the phenomena are no longer isothermic (melting of an alloy, crossing of a two-phase domain etc.).

For example, the $T_{solidus}$ of an alloy $A_{1-x}B_x$ has to be taken as $T_{solidus} = T_0$ and $T_{liquidus}$ as $T_{liquidus} = T_{fin} - (\Delta T_{fin})_0$, x. If $(\Delta T_{fiin})_A$ and $(\Delta T_{fin})_B$ are not

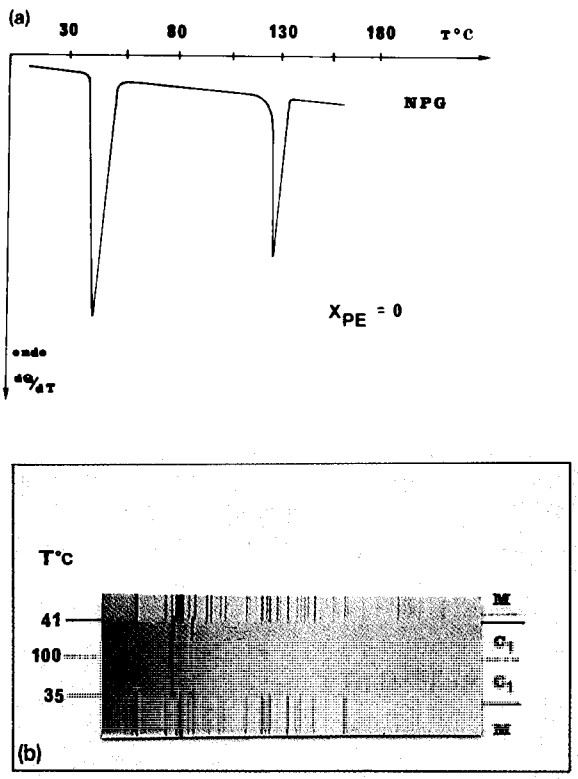

Fig. 1. NPG: (a) recorded thermogram; (b) Guinier–Simon pattern.

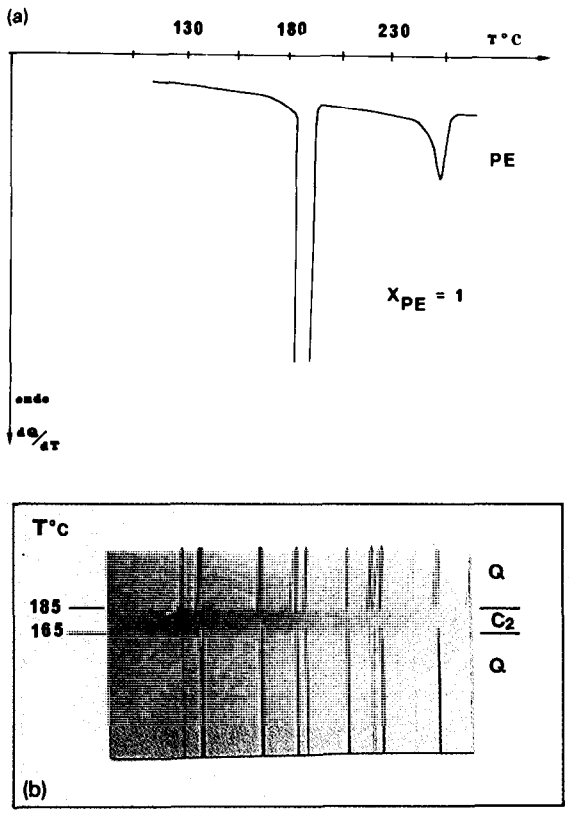

Fig. 2. PE: (a) recorded thermogram; (b) Guinier–Simon pattern.

absolutely identical (within the experimental margin of error) a linear interpolation may be taken. This has been done hereafter.

Figures 1a and 2a show the recorded thermograms for the pure compounds NPG and PE, and Figs. 1b and 2b the corresponding Guinier–Simon patterns.

A first look at the thermograms for the composition range extending from $X_{PE} = 0.03$ to $X_{PE} = 0.95$ indicates the presence of an invariant level (eutectoid invariant FGH) for a mean temperature of 36 °C. In the low temperature part, Guinier–Hägg observations confirmed for this concentration domain the coexistence of monoclinic (M) and quadratic (Q) solid solutions. Above 36 °C the monoclinic solid solution transforms to a cubic C_1 solid solution.

A liquidus line for the diagram $T = f(X_{PE})$ may be built from thermogram analysis, as well as two invariant lines at the temperatures lying near 163 °C (peritectic invariant F′G′H′) and 172 °C (metatectic invariant F″G″H″). In order to investigate thoroughly all details revealed by DSC analysis we have to acquire further information as to phase transformations with temperature.

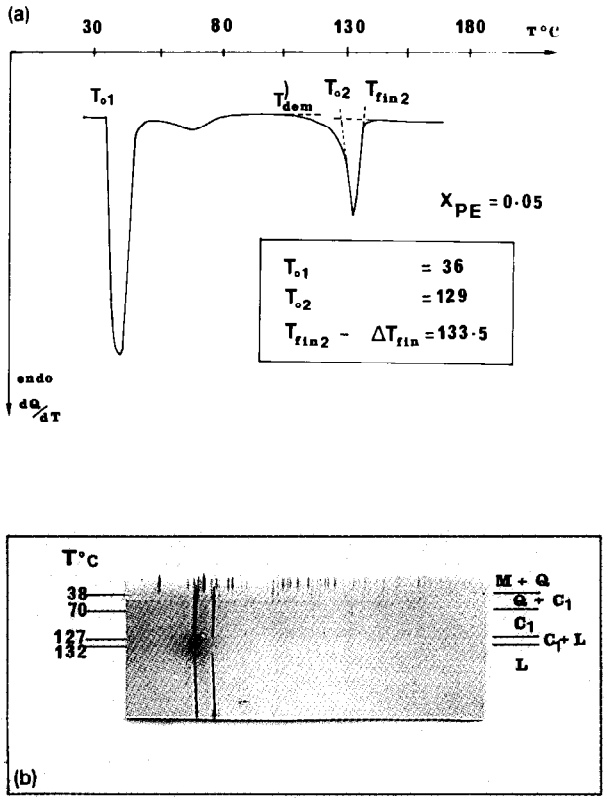

Fig. 3. NPG–PE system ($X_{PE} = 0.05$): (a) recorded thermogram; (b) Guinier–Simon pattern.

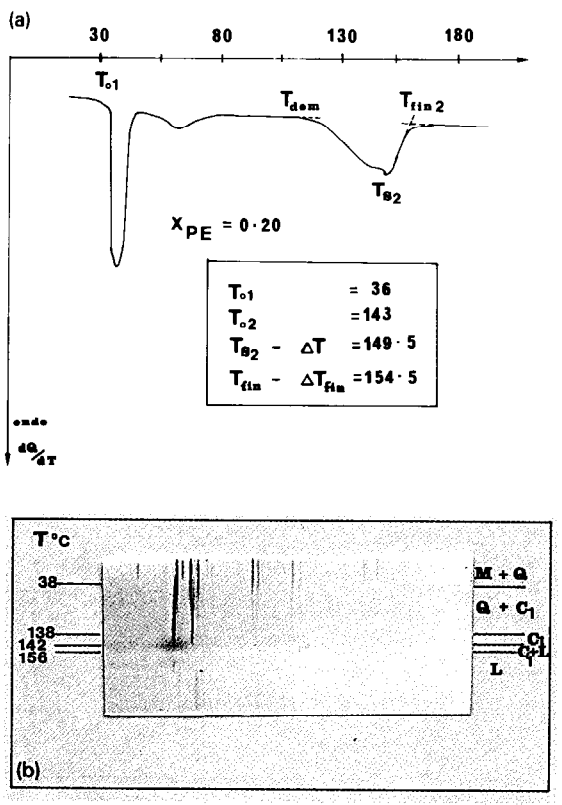

Fig. 4. NPG–PE system ($X_{PE} = 0.20$): (a) recorded thermogram; (b) Guinier–Simon pattern.

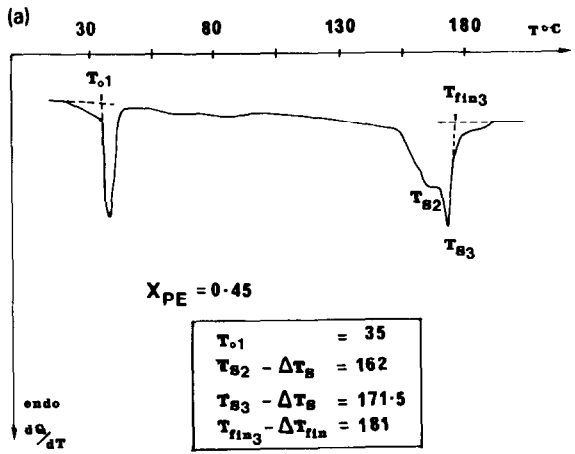

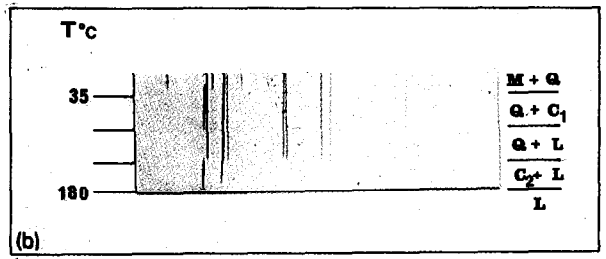

Fig. 5. NPG–PE system ($X_{PE} = 0.45$): (a) recorded thermogram; (b) Guinier–Simon pattern.

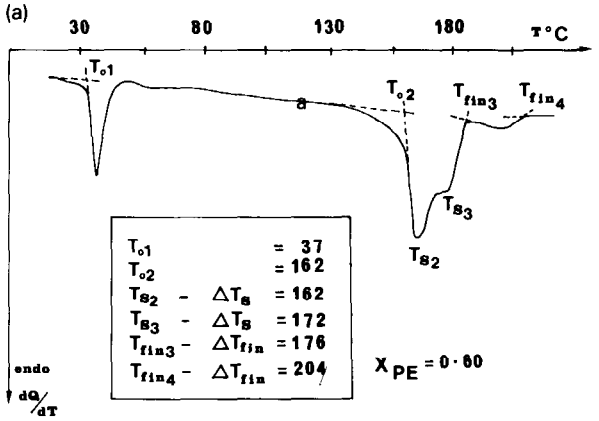

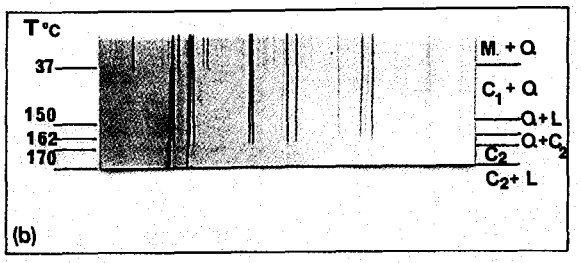

Fig. 6. NPG–PE system ($X_{PE} = 0.60$): (a) recorded thermogram; (b) Guinier–Simon pattern.

Figures 3 and 4 give thermograms and Guinier–Simon patterns for $X_{PE} = 0.05$ and $X_{PE} = 0.20$ samples. For these two concentrations, as temperature rises, one meets successively the following:

existence of a two-phase domain M + Q;
disappearance of M and appearance of C_1 at $T = 36\,°C$;
existence of a two-phase domain C_1 + Q;
crossing of the boundary of a miscibility gap (Q disappears at $T = T_{dem}$);
existence of a one-phase domain C_1;
beginning of melting;
existence of a two-phase domain C_1 + L;
end of melting;
existence of a one-phase domain L.

Figures 5 and 6 pertain to $X_{PE} = 0.45$ and 0.60 and these compositions are representative of the two situations encountered for samples with X_{PE} compositions between 0.40 and 0.70.

For $X_{PE} = 0.45$, the successive domains may be described as,
existence of a two-phase domain M + Q,
disappearance of M and appearance of C_1 at $T = 36\,°C$,

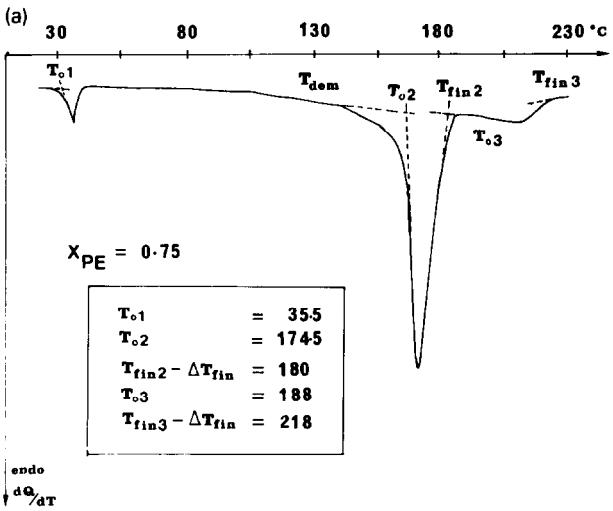

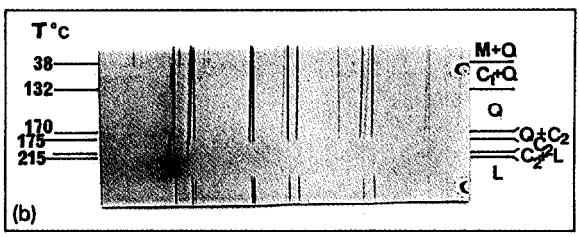

Fig. 7. NPG–PE system ($X_{PE} = 0.75$): (a) recorded thermogram; (b) Guinier–Simon pattern.

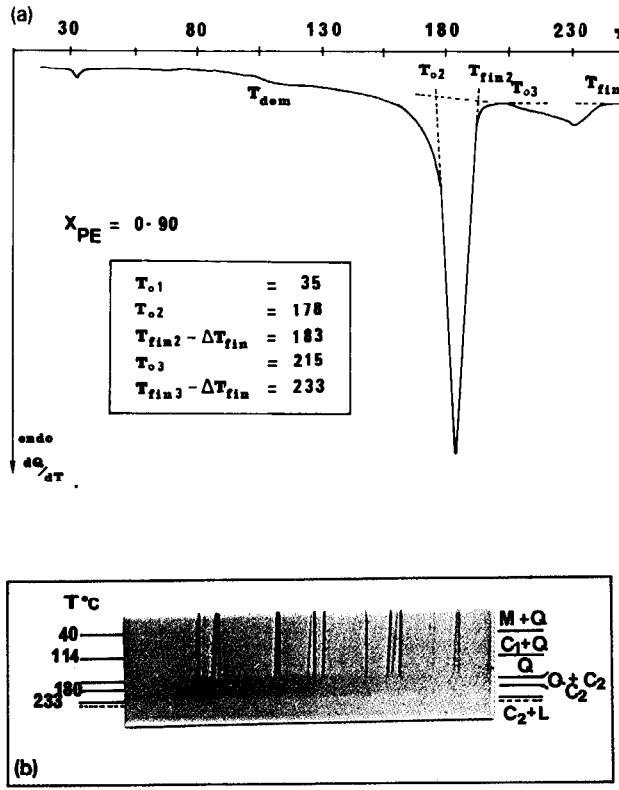

Fig. 8. NPG–PE system ($X_{PE} = 0.90$): (a) recorded thermogram; (b) Guinier–Simon pattern.

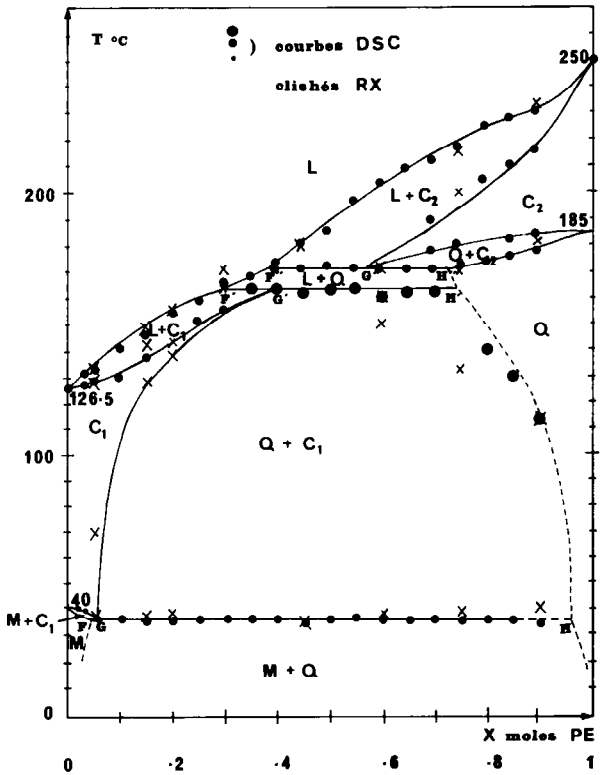

Fig. 9. Proposed phase diagram for NPG–PE system.

existence of a two-phase domain $C_1 + Q$,
disappearance of C_1 and appearance of liquid L at $T = 163°C$,
existence of a two-phase domain $L + Q$,
disappearance of Q and reappearance of C_1 at $T = 172°C$,
existence of a two-phase domain $L + C_1$
end of the melting at $T = 181°C$,
existence of a one-phase domain L.
For $X_{PE} = 0.60$, we observed the following steps:
existence of a two-phase domain $M + Q$;
disappearance of M and appearance of C_1 at $T = 36°C$;
existence of a two-phase domain $C_1 + Q$;
disappearance of C_1 and appearance of liquid L, $T = 163°C$;
existence of a two-phase domain $L + Q$;
disappearance of L and and appearance of a cubic phase C_2 at $T = 172°C$;
existence of a two-phase domain $C_2 + Q$;

TABLE 1

Corrected temperatures recorded from DSC experiments on the binary NPG–PE system [a]

X_{PE} (mol.%)	T_1 (°C)	T_2 (°C)	T_3 (°C)	T_4 (°C)	T_5 (°C)	T_6 [b] (°C)	T_7 [c] (°C)
0.00	40					126.5	126.5
0.03	37					128	130
0.05	36					129	133.4
0.10	36					130	140
0.15	36					138	146.5
0.20	36					143	154.5
0.25	35.5					152	159.5
0.30	36					156	166.8
0.35	36.5	163.5					168.6
0.40	36.5	163.5	171				173.4
0.45	35	162	171.5				181
0.50	36.5	164.5	172.5				186
0.55	37	164.5	173				198
0.60	37	162	172		176		204
0.65	35	163	172				209
0.70	35	163.5	171.5		178	186	212
0.75	35			174.5	180	188	218
0.80	35.5			175	182	205	225
0.85	36			176	182	210	228
0.90	34			178	183	215	232
1.00				185	185	250	250

[a] T_1, temperature for NPG transition and eutectoid invariant; T_2, peritectic invariant; T_3, metatectic invariant; T_4, beginning of quadratic/cubic transition; T_5, end of quadratic/cubic transition; T_6, beginning of melting, $T_{solidus}$. T_7, end of melting.

[b] "$T_{solidus}$" for simplicity.

[c] $T_{liquidus}$.

disappearance of Q at $T = 176\,^{\circ}C$;
existence of a one-phase domain C_2;
beginning of the melting of C_2 at $T = 178\,^{\circ}C$;
existence of a two-phase domain $L + C_2$;
end of the melting of C_2 at $T = 204\,^{\circ}C$;
existence of a one-phase domain L.

These facts support the existence of a metatectic phenomenon following a peritectic one, the metatectic point being located between $X_{PE} = 0.45$ and $X_{PE} = 0.60$ (more precisely around $X_{PE} = 0.55$).

This explanation stands for further analysis of compositions $X_{PE} = 0.75$ and $X_{PE} = 0.90$ presented in Figs. 7 and 8. In both cases, we obtain the following features:

existence of a two-phase domain M + Q;
disappearance of M and appearance of C_1 at $T = 36\,^{\circ}C$;
existence of a two-phase domain $C_1 + Q$;
crossing of a demixtion line;
existence of a one-phase domain Q;
existence of a two-phase domain $Q + C_2$;
existence of a one-phase domain C_2;
existence of a two-phase domain $L + C_2$;
existence of a one-phase domain L.

Table 1 gives all the experimental characteristic temperatures recorded from thermogram analysis. Figure 9 shows the proposed phase diagram, accounting for most of our experimental observations.

REFERENCES

1 J. Timmermans, J. Phys. Chem. Solids, 18 (1961) 1.
2 C.P. Smyth, Chem. Rev., 19 (1936) 329.
3 G.B. Guthrie and J.P. McCullough, J. Phys. Chem. Solids, 18 (1961) 53.
4 N. Boden, in J.N. Sherwood (Ed.), The Plastically Crystalline State, Wiley, 1979.
5 R. Rudman, Solid State Commun., 29 (1979) 785.
6 E. Murrill and L. Breed, Thermochim. Acta, 1 (1970) 239.
7 T.L. Vigo and C.M. Frost, Thermochim. Acta, 76 (1984) 333.
8 D.K. Benson, R.W. Burrows and C.D. Shinton, U.S. Patent 4, 572, 864 (23-2-1986).
9 D.K. Benson, R.W. Burrows and J.D. Webbs, Solar Energy Mater., 13 (1986) 133.
10 L.A. Staveley, Annu. Rev. Phys. Chem., 13 (1961) 351.
11 D.K. Benson, SERI Rep., 255/DRAFT/MRB770, July 1987, personal communication.
12 M. Barrio, J. Font, J. Muntasell, J.L. Tamarit, N.B. Chanh and Y. Haget, J. Chim. Phys, 87 (1990) 255.
13 M. Teisseire, Doctorate Thesis, University of Nice, Nov. 1989.
14 J.L. Tamarit, Doctorate Thesis, Polytechnic School of Barcelona, 1988.
15 R. Courchinoux, N.B. Chanh, Y. Haget, T. Calvet, E. Estop and M.A. Cuevas-Diarte, J. Chim. Phys. 86 (1989) 562.
16 International Conference on Thermal Analysis Standardisation Committee, J. Thermal. Anal., 7 (1975) 695.